



Published in final edited form as:

J Pharm Biomed Anal. 2015 March 25; 107: 518–525. doi:10.1016/j.jpba.2015.01.036.

***N*-Acetyl-*S*-(*N,N*-diethylcarbamoyl) cysteine in rat nucleus accumbens, medial prefrontal cortex, and in RAT and human plasma after disulfiram administration**

Robert D. Winefield^{a,**}, Anthonius A.M. Heemskerk^{b,1}, Swetha Kaul^{c,2}, Todd D. Williams^a, Michael J. Caspers^d, Thomas E. Prisinzano^d, Elinore F. McCance-Katz^{e,3}, Craig E. Lunte^d, and Morris D. Faiman^f

^aMass Spectrometry Laboratory, University of Kansas, Lawrence, KS 66045, USA

^bDepartment of Pharmaceutical Chemistry, University of Kansas, Lawrence, KS 66047, USA

^cRalph N. Adams Institute for Bioanalytical Chemistry, Department of Chemistry, University of Kansas, Lawrence, KS 66045, USA

^dDepartment of Medicinal Chemistry, University of Kansas, Lawrence, KS 66045, USA

^eDepartment of Psychiatry, University of California, San Francisco, San Francisco, CA 94143, USA

^fDepartment of Pharmacology and Toxicology, University of Kansas, Lawrence, KS 66045, USA

Abstract

Disulfiram (DSF), a treatment for alcohol use disorders, has shown some clinical effectiveness in treating addiction to cocaine, nicotine, and pathological gambling. The mechanism of action of DSF for treating these addictions is unclear but it is unlikely to involve the inhibition of liver aldehyde dehydrogenase (ALDH2). DSF is a pro-drug and forms a number of metabolites, one of which is *N*-acetyl-*S*-(*N,N*-diethylcarbamoyl) cysteine (DETC-NAC). Here we describe a LCMS/MS method on a QQQ type instrument to quantify DETC-NAC in plasma and intracellular fluid from mammalian brain. An internal standard, the *N,N*-diisopropylcarbamoyl homolog (MIM: 291 > 128) is easily separable from DETC-NAC (MIM: 263 > 100) on C18 RP media with a methanol gradient. The method's linear range is 0.5–500 nM from plasma and dialysate salt solution with all precisions better than 10% RSD. DETC-NAC and internal standards were recovered at better than 95% from all matrices, perchloric acid precipitation (plasma) or formic acid addition (salt) and is stable in plasma or salt at low pH for up to 24 h. Stability is observed through three freeze-thaw cycles per day for 7 days. No HPLC peak area matrix effect was greater

© 2015 Published by Elsevier B.V.

Correspondence to: Morris D. Faiman.

** Corresponding author. Present address: Analytical Core Laboratory, Department of Pharmacology, Toxicology and Therapeutics, University of Kansas Medical Center, Kansas City, KS 66160, USA, Tel.: +1 9135884762, fax: +1 9135887501, rwinefield@kumc.edu (R.D. Winefield)

¹Present address: Center for Proteomics and Metabolomics, Leiden University Medical Center, Leiden, The Netherlands.

²Present address: Allergan Inc., Irvine, CA 92612, USA.

³Present address: Substance Abuse and Mental Health Services Administration, Rockville, MD 20857, USA.

Appendix A. Supplementary data: Supplementary data associated with this article can be found, in the online version, at <http://dx.doi.org/10.1016/j.jpba.2015.01.036>.

than 10%. A human plasma sample from a prior analysis for *S*-(*N,N*-diethylcarbamoyl) glutathione (CARB) was found to have DETC NAC as well. In other human plasma samples from 62.5 mg/d and 250mg/d dosing, CARB concentration peaks at 0.3 and 4 nM at 3 h followed by DETC-NAC peaks of 11 and 70 nM 2 h later. Employing microdialysis sampling, DETC-NAC levels in the nucleus accumbens (NAc), medial prefrontal cortex (mPFC), and plasma of rats treated with DSF reached 1.1, 2.5 and 80 nM at 6 h. The correlation between the appearance and long duration of DETC-NAC concentration in rat brain and the persistence of DSF-induced changes in neurotransmitters observed by Faiman et al. (Neuropharmacology, 2013, 75C, 95–105) is discussed.

Keywords

Disulfiram; *N*-acetyl-*S*-(*N,N*-diethylcarbamoyl) cysteine; DETC-NAC; Carbamathione; Substance abuse disorders; Mercapturate pathway

1. Introduction

Disulfiram (DSF; PubChem CID: 3117), originally identified as a treatment for alcohol addiction [1], has now been found to also have potential for the treatment of several other substance use disorders. These include addiction to cocaine [2,3], nicotine [4], marijuana [5] and the behavioral addiction pathological gambling [6,7]. The pharmacological basis for DSF's use in alcohol addiction is its ability to inhibit liver mitochondrial aldehyde dehydrogenase (ALDH₂) [1]. While the mechanism by which DSF acts to treat non-alcoholic substance abuse disorders and pathological gambling behaviors is unclear, it is unlikely to involve the inhibition of ALDH₂.

DSF is a pro-drug that is metabolized to a number of metabolites (Fig. 1). The metabolic pathways, including the drug metabolizing enzymes identified in DSF's bioactivation, have been described previously [8–11]. *S*-methyl diethyldithiocarbamate sulfoxide (DETC-MeSO) (Fig. 1) is the DSF metabolite that inhibits ALDH₂ [12,13] and it is also believed to be responsible for the disulfiram–ethanol reaction seen in DSF-treated patients after ethanol ingestion. The carbamoylation of glutathione by DETC-MeSO leads to the formation of *S*-(*N,N*-diethylcarbamoyl) glutathione (CARB) (Fig. 1) [14,15].

CARB is found in the bile of rats after the administration of either DSF or diethyldithiocarbamate (DDTC) [15] and in the plasma of human volunteers treated with DSF [16]. In microdialysis studies in rats, CARB is found in the nucleus accumbens (NAc) shell, and in plasma of rats following intraperitoneal DSF administration [17]. When CARB is administered intravenously, CARB is found in the medial prefrontal cortex (mPFC) in addition to the NAc and plasma. In the brain, CARB administration increases dopamine, decreases gamma-aminobutyric acid and has a biphasic effect on glutamate. Similar findings were observed in rats following intraperitoneal DSF administration. These effects were absent in rats concurrently administered DSF and *N*-benzylimidazole, a cytochrome P450 inhibitor. Inhibition of DSF bioactivation blocks the formation of DSF-metabolites while attenuating any changes in these neurotransmitters [17]. Of interest is that after CARB administration, CARB disappears rapidly (half-life of approximately 4 min) from the NAc,

mPFC, and plasma. Yet, changes in dopamine, gamma-aminobutyric acid, and glutamate persist for almost 2-h. Although the reason for this is not readily apparent, one explanation could be the formation of another bioactive metabolite downstream from CARB (Fig. 1).

In previous studies Heemskerk et al. [16] observed both CARB and an unidentified peak in the plasma (Fig. 2A) of human volunteers treated with DSF. Preliminary mass spectrometry studies suggested that the unidentified peak was *N*-acetyl-*S*-(*N,N*-diethylcarbamoyl) cysteine (DETC-NAC; Fig. 2B). Additionally, Hu et al., [18] found DETC-NAC in the urine of rats treated with either DSF or diethyldithiocarbamate (DDTC) and Nagendra and Faiman (unpublished results) detected DETC-NAC in urine from rats treated with DETC-MeSO. These observations are consistent with the metabolic elimination of DETC-MeSO through the mercapturate pathway – a means by which potentially toxic alkylating agents are eliminated [19]. Because DETC-NAC is the result of the *S*-carbamoylation of glutathione by DETC-MeSO, (e.g. the formation of CARB) DETC-NAC is probably the product of the mercapturate pathway. However, that DETC-NAC is produced in the liver and kidneys as part of phase II metabolism does not explain the presence of CARB and (potentially) DETC-NAC in the mammalian brain.

To better understand this juxtaposition of DSF metabolites and neurotransmitter transmitter changes [17], studies were carried out to firstly, identify the aforementioned unknown peak as DETC-NAC (Fig. 2A) and secondly, to design a HPLC– or UHPLC–MS/MS methodology appropriate for quantifying DETC-NAC in human plasma, and in the NAc, mPFC, and plasma of rats. The present findings are the first report identifying DETC-NAC in plasma from human volunteers treated with DSF and the appearance of DETC-NAC in the NAc and mPFC and in plasma from rats after DSF administration. The finding of DETC-NAC in the NAc and mPFC, two brain regions associated with the reward pathway, may provide a rationale for the use of DSF in the treatment of several substance abuse disorders such as cocaine abuse, nicotine abuse, and the behavioral addiction pathological gambling.

2. Methods and materials

2.1. Chemicals and reagents

The artificial cerebrospinal fluid solution was prepared as previously described [20]. Components of the artificial cerebrospinal fluid solution, formic acid, perchloric acid (70%, w/v), and HPLC grade methanol were purchased from Fisher (Fairlawn, NJ, USA). Ammonium bicarbonate, *N*-acetyl-*L*-cysteine, diethylcarbamoyl chloride and *N,N*-diisopropylcarbamoyl chloride were purchased from Sigma–Aldrich (St. Louis, MO, USA). Ketamine was purchased from Fort Dodge Animal Health (Fort Dodge, IA, USA) and xylazine was purchased from Lloyd Laboratories (Shenandoah, IA, USA). Nanopure water was prepared using a Water Pro Plus purification system (Labconco, Kansas City, MO, USA). Blank pooled human plasma was purchased from Innovative Research (Novi, MI, USA).

2.2. Synthesis of DETC-NAC and DIPC-NAC

DETC-NAC and *N*-acetyl-*S*-(*N,N*-di-isopropylcarbamoyl) cysteine (DIPC-NAC) were synthesized by the same method: 1 g diethylcarbamoyl chloride or *N,N*-diisopropylcarbamoyl chloride dissolved in 35 mL of pyridine was added to an 8 mL aqueous solution of *N*-acetyl-L-cysteine (0.33 g, 2.02 mmol) over 5 minutes at 0 °C. The mixture was stirred overnight at 25 °C and then concentrated in vacuo. The residual paste was purified by flash column chromatography using a methanol: ethyl acetate solvent mixture specific to each product. Product fractions were concentrated in vacuo to generate a milky white solid.

The structure of DETC-NAC and DIPC-NAC was confirmed, in each case by triplicate exact mass determinations and ¹H, ¹³C NMR experiments. The exact mass of DETC-NAC ([M+H]⁺, C₁₀H₁₉N₂O₄S, theoretical exact mass: 263.1066) was 263.1063 ± 0.0036, -1.14 ppm from the theoretical mass. The exact mass of DIPC-NAC ([M+H]⁺ C₁₂H₂₃N₂O₄S theoretical exact mass: 291.1379) was 291.1408 ± 0.00056, +2.9 ppm from the theoretical mass. DETC-NAC purified by flash column chromatography (5:95 methanol:ethyl acetate) produced a white solid (68.2%). Spectral data matched previously reported results [18].

DIPC-NAC, purified by flash column chromatography (3:97 methanol:ethyl acetate) produced a white solid (62.8%). ¹H NMR (500 MHz, deuterium oxide) δ 4.39 (dd, *J* = 8.6, 4.0 Hz, 1H), 4.17 (d, *J* = 11.7 Hz, 1H), 3.65 (s, 1H), 3.42–3.35 (m, 1H), 3.10 (ddd, *J* = 14.2, 8.6, 0.8 Hz, 1H), 1.99 (d, *J* = 0.7 Hz, 3H), 1.34–1.15 (m, 13H). ¹³C NMR (126 MHz, deuterium oxide) δ 176.32, 173.44, 166.93, 54.77, 50.47, 47.32, 31.71, 21.90, 19.82, 19.21.

2.3. Analytical methods

2.3.1. LC method for UV and mass spectrometric detection—HPLC–UV (HPLC coupled to a UV/visible detector) experiments were performed modifying the method of Heemskerk et al. [16] with three alterations. (1) The HPLC was a Waters Alliance 2695 (Waters Co., Milford, MA, USA) equipped with a Waters 2487 absorbance detector set to 215 nm controlled with Waters Mass-Lynx 4.1 software. (2) An alternate guard column (2 mm × 20 mm guard column packed, in-house, with 5 μm SB-C18 Agilent Zorbax resin; Agilent Technologies, Santa Clara, CA, USA) was used to protect the resolving column. (3) HPLC mobile phase: solvent A consisted of water, methanol and formic acid (99:1:0.1, v/v/v) while solvent B consisted of methanol, water and formic acid (99:1:0.1, v/v/v). The sample (50 μL) was loaded at 15% B and a linear gradient (3% B/min rate of change, 500 μL/min flow rate) ending at 80% B was used to resolve the analytes. Between injections, the column was re-equilibrated at 5% B for 3-min. For HPLC–MS/MS, HPLC-columns and mobile phase compositions used in the experiments are as described in Heemskerk et al. [16] on a Waters Acquity chromatograph with a Phenomenex Kinetex column (phase C18; diameter, 2.1 mm × 50 mm; particles size, 1.7 μm; pore size, 100 Å). The HPLC-gradient was altered as follows: The sample was loaded onto the column using a 50 μL injection volume at 5% B and was resolved in a 6-min gradient of 11% B per minute then to 90% B at 400 μL/min. The first 2 min of gradient was diverted to waste and between injections, the column was washed for 2-min at 80% B and re-equilibrated at 5% B for 1.5-min.

2.3.2. Mass spectrometric conditions—Mass spectrometry was performed using the parameters described by Heemskerk et al. [16] on a Micromass Quattro Ultima (Micromass Ltd. Manchester, UK). Optimal cone voltage and collision energies were 35 V and 15 V for DETC-NAC and 35 V and 10 V respectively for DIPC-NAC. Voltages and collision energies used to detect CARB were identical to those used by Heemskerk et al. [16]. Data processing was performed using Waters MassLynx 4.1 and GraphPad Prism 5 (GraphPad Software Inc., La Jolla, CA, USA).

2.4. Stability assay

The stability of DETC-NAC was studied under a number of analysis and storage conditions. The stability at low pH was assessed in quintuplicate using a protein-free extract of plasma (protein was removed by perchloric acid-mediated protein precipitation) spiked with 150 μM DETC-NAC. The samples were incubated at room temperature and sampled at 2-, 4-, 6- and 24-h prior to analysis by HPLC–UV. The stability of DETC-NAC before and after precipitation was tested in a similar way using aliquots of pooled human plasma aliquots spiked with 150 μM DETC-NAC. Quintuplicate plasma aliquots were allowed to incubate at room temperature for 2-, 4-, 6- and 24-h before sample pretreatment and analysis. The stability in storage conditions was assessed by analyzing 150 μM spiked plasma after three freeze thaw cycles and at 1-, 3- and 7-days after storage at $-20\text{ }^{\circ}\text{C}$. External calibration of DETC-NAC was performed using five point calibration curves of 50 μM –250 μM in plasma; a calibration range selected to accommodate the large DETC-NAC concentration used specifically in this stability assay.

2.5. Validation of quantitative HPLC–MS/MS assay

Matrix-induced suppression of DETC-NAC ionization was assessed using a post-column infusion method described previously [21]. Briefly DETC-NAC was infused post-column into the HPLC eluent stream entering the mass spectrometer. In MIM mode, DETC-NAC's 263 > 100 transition were monitored while pre-treated, DETC-NAC free, plasma samples were resolved by the HPLC-column. No significant matrix-induced suppression of DETC-NAC ionization was indicated by this method. The intra and inter-day stability of the method was quantitatively assessed by comparing calibration curves produced on each of four consecutive days. The standard curves were produced by analyzing plasma samples spiked with 1.0, 5.0, 10.0, 50.0, and 100.0 nM DETC-NAC. The linearity of the method was successfully determined out to 500 nM.

2.6. In vivo studies

2.6.1. Human studies—Two human studies were carried using a subset of samples from a study of patients receiving disulfiram. The first analysis was to confirm that DETC-NAC was formed after the administration of DSF to a healthy volunteer as suggested from our previous studies [16] (Fig. 2A and B). In those studies a female volunteer weighing 69 kg and 160 cm in height without any substance use disorder was recruited. DSF (250 mg/day) was given for 3-days. On the fourth day (24-h after the last dose of DSF and after an 8-h overnight fast) after an overnight fast, an antecubital venipuncture was carried out and blood drawn to obtain a base-line drug concentration at zero time (t_0). A dose of DSF was then

administered and blood drawn 1-, 2-, 4-, 6-, 8-, and 10-h after DSF dosing. The 2-h time point was selected to evaluate the analytical method developed for DETC-NAC (Figs. 2B, 3, and 4). The procedures used and patient characteristics are described in the previous study (Fig. 2A and B) [16].

The second analysis was carried out to determine the plasma concentration-time profile for DSF administered to three healthy volunteers (without substance use disorders) at two different doses, these being 62.5 mg/day and 250 mg/day (Fig. 5A and B). Disulfiram 62.5 mg/day was administered with staff observation for 3-days. On the fourth day, (24-h after the last dose of DSF and after an 8-hour overnight fast) an antecubital venipuncture was performed and 7 mL of blood drawn into a heparinized tube to obtain a baseline plasma DETC-NAC concentration at t_0 . A urine sample also was collected prior to DSF dosing which was negative for recent use of illicit substances (opiates, cocaine, amphetamines, marijuana and benzodiazepines). The 62.5 mg dose of DSF was then administered and blood samples drawn at 1-, 2-, 4-, 8-, 10-, and 12-h after DSF dosing. This was followed by a 4-day wash out period. This identical protocol was then repeated with a dose of 250 mg/day DSF. After each blood draw, and for each dose studied, the blood sample was immediately centrifuged, separated, and the plasma was frozen at $-70\text{ }^{\circ}\text{C}$ until analysis could be carried out.

In both healthy subject studies, voluntary, written, and informed consent was obtained. The study was reviewed and approved by the Institutional Review Board at the University of California, San Francisco (UCSF).

2.7. Rat studies

2.7.1. Animals and surgeries—Male Sprague–Dawley rats (Charles River Laboratories, Wilmington, MA) weighing between 300 and 400 g were used. The rats were housed in a temperature and humidity controlled facility (University of Kansas Animal Care Unit, Lawrence, KS, USA) maintained on a 12-h light/dark cycle with access to food and water ad libitum. Twenty-four hours before initiating the studies, the rats were brought into the laboratory, housed individually, and acclimated. All microdialysis studies were carried out during the light phase. Prior to surgery, the rats were anesthetized employing isoflurane inhalation, and given a subcutaneous mixture of ketamine, xylazine, and acepromazine. The anesthetic doses, and animal preparation for surgery have been described previously [20].

DSF was administered via a recently developed an intraperitoneal method that minimizes animal handling [17]. Plasma samples were collected using an intravenous PE-10 cannula implanted into the external femoral vein as described by Kaul et al. [20].

2.7.2. Rat microdialysis and rat plasma studies—The infusion pump and fraction collector installation as well as the exact manner by which microdialysis probes were implanted into rat brains for NAc and mPFC measurements and the jugular vein for plasma measurements has been described previously [17]. Briefly, holes were drilled through the skull. Guide cannulas were positioned 2 mm above the NAc and mPFC, and then replaced with microdialysis probes. Coordinates relative to the bregma were +1.5 mm anterior, +0.9

mm lateral, and -6.2 mm ventral for the NAc shell and +3.7 mm anterior, +0.7 mm lateral, and -1.0 mm ventral for the mPFC [22]. A microdialysis probe was inserted into the jugular vein for sampling of plasma DETC-NAC. Post-surgery sample collection, DSF preparation, DSF administration, and brain harvesting procedures were performed as described by Faiman et al. [17]. Post-surgery, brain and vascular probes were perfused (2 μ L/min) with the artificial cerebrospinal fluid solution and Ringer's solution respectively. Sample collection was initiated 24-h after surgery similar to a previously used procedure [23].

DSF (200 mg/kg) was prepared as a suspension in saline, sonicated, and the suspension administered through the specially prepared intraperitoneal cannula. Microdialysis samples were collected every 15-min for 6-h. Following the experiment, the rats were killed and their brains removed, fixed in 10% (v/v) formalin, embedded in paraffin wax and sectioned for histological confirmation of probe placement using procedures previously described [17]. Only probes which exhibited at least 85% of active dialysis membrane in the NAc shell and the mPFC were included for analysis.

All animal experiments were conducted in accordance with guidelines established by the Institutional Animal Care and Use Committee at the University of Kansas. Experiments were carried out in accordance with NIH guidelines and met AAALAC standards.

2.8. Determination of DETC-NAC in plasma and brain dialysate

2.8.1. HPLC-MS/MS sample preparation—DETC-NAC and DIPC-NAC stock solutions were made at 1 mM concentrations in 100 mM ammonium bicarbonate buffer. CARB and *S*-(*N,N*-di-*n*-propylcarbamoyl) glutathione (homologous internal standard for CARB) solutions were prepared and diluted as described in Heemskerk et al. [16]. Calibrant solutions were prepared from these stock solutions using either water or Ringer's solution for quantitation of DETC-NAC or CARB or both in dialysate.

DETC-NAC concentrations in dialysate samples were quantified using a five point calibration curve derived from quintuplicate Ringer's solutions spiked with 1.0, 5.0, 10.0, 50.0 and 100.0 nM of DETC-NAC. Prior to HPLC-MS/MS analysis of dialysate samples, 40 μ L of 1% (v/v) formic acid per 20 μ L of dialysate sample to increase the volume of sample for the auto injector and, presumably, enhance or preserve chromatographic focusing.

An internal standard, DIPC-NAC, was incorporated into all plasma and calibrant samples. Human plasma, 100 μ L aliquot, was supplemented with 55 μ L of water, 10 μ L of DIPC-NAC solution (100 nM) and the mixture vortexed for 5 s. For calibration, the proportions were modified as follows: 100 μ L of plasma, 45 μ L water, 10 μ L of DIPC-NAC (100 nM) and 10 μ L of a DETC-NAC calibration stock solution. Plasma proteins in both sample and standard mixtures were precipitated by the addition of 35 μ L perchloric acid (5 s vortex, 5 min incubation at 0 $^{\circ}$ C) and the precipitate was discarded after centrifugation (5 min, 11,000 \times g, 25 $^{\circ}$ C). The supernatant was retained and analyzed.

2.8.2. Microdialysis probe calibration—The characteristics of the implanted microdialysis probes were evaluated at the end of each experiment. Based upon triplicate

experiments, the in vivo extraction efficiency for DETC-NAC was as follows (mean \pm standard error): $53.7 \pm 9.8\%$ for the brain probes and $81.3 \pm 10.8\%$ for the plasma vascular probe.

3. Results and discussion

3.1. DETC-NAC identified in previous study

We investigated the unidentified peak (Fig. 2A) described by Heemskerk et al. [16] by re-running the patient plasma sample in question. The HPLC–MS/MS conditions used were identical to Heemskerk et al. [16] except for the addition of a DETC-NAC specific $263 > 100$ Da transition that we identified through empirical examination of the DETC-NAC specific collision-induced disassociation spectrum (Fig. 3A). As shown in Fig. 2B, the unknown peak was explicitly identified as DETC-NAC based on their identical chromatographic retention times. This led us to develop a DETC-NAC specific quantitation method to facilitate clinical studies of this DSF metabolite.

3.2. Quantitation of DETC-NAC: method development

3.2.1. Internal standard selection—Robust LC–MS/MS based quantification requires an internal standard closely matching the solubility, chemical activity, ionization and structure of the intended analyte as closely as practically possible [24]. Because it was impractical to purchase a stable isotope mimic of the analyte or to synthesize one using isotope-labeled precursors, we chose to synthesize DIPC-NAC, a close structural relative of DETC-NAC. This strategy was similar to that employed previously by Heemskerk et al. [16].

The collision-induced dissociation spectra of both DETC-NAC and DIPC-NAC were examined and we determined that the most abundant MIM transitions corresponded to the carbamoyl fragment from both molecules. For DETC-NAC this transition is $263-100$ u (Fig. 3A) and for DIPC-NAC, this transition is $291-128$ u (Fig. 3B).

3.2.2. HPLC conditions—Our DETC-NAC HPLC–MS/MS quantitation method is an adaptation of the CARB specific LC-methodology developed by Heemskerk et al. [16]. We retained, for the same reasons, their choice in LC-column technology and large (50 μ L) sample loading volumes. We modified their LC-gradient as follows: (1) an analyte focusing phase with 5% methanol, (2) a gradient elution of 11%/min increase of solvent B (99% methanol), (3) a washing phase of 80% solvent B, and (4) a re-equilibration phase at the initial conditions. The typical selectivity and sensitivity of this HPLC–MS/MS method can be seen in Fig. 4.

3.2.3. Addressing: (1) ion suppression, (2) recovery, and (3) stability

1. Matrix-based ion-suppression of DETC-NAC and DIPC-NAC was assessed by a post-column infusion assay described previously [16]. There was no indication (e.g. peak area change of greater than 10%) that either analyte-ion suffered suppression during the relevant chromatographic retention times.

2. The fact that perchloric acid-mediated protein precipitation is a routine method for extracting and concentrating either acidic-or neutral drugs from biological matrices [5] notwithstanding, we evaluated our ability to quantitatively recover DETC-NAC from perchloric acid-treated plasma samples by quantifying DETC-NAC detected (after incubation) in DETC-NAC spiked samples prepared in either plasma or water. The mean analytical recovery $99.1 \pm 3.3\%$ demonstrates that DETC-NAC is stable both in the presence of perchloric acid and at 21 °C for at least 24-h (Table S1).
3. The destabilizing effects of freeze-thaw events on DETC-NAC were assessed by subjecting spiked samples to three freeze-thaw cycles and storage at -20 °C for up to 7 days. No significant degradation was observed (Table S2).

3.2.4. Linearity, accuracy, precision and limits of quantitation—The linearity and accuracy of this method was assessed by generating calibration curves from quintuplicate samples comprised of blank pooled human plasma spiked with DETC-NAC. As can be seen in Table S3, acceptable levels of accuracy, within 5% of expectation, precision (within 10% over the 1 nM–500 nM range), and linearity were achieved. These levels were maintained when the inter-day repeatability of the method was assessed by the generation of calibration curves covering the 1.0 nM–100.0 nM range over four successive days. The limit of quantitation was not determined below 1 nM as this concentration was adequate for subsequent analyses.

3.2.5. Determination of DETC-NAC in human plasma—The utility of this LC–MS method in humans was examined. Three volunteers were given two separate doses of DSF in a crossover study (Fig. 5) After an oral dose of 62.5 mg of DSF, an average lag of approximately 1-h was observed before a significant concentration of DETC-NAC appeared in the plasma of each patient (Fig. 5A). This lag period is due to not only the delay in stomach emptying time, but also to the poor solubility and absorption characteristics of DSF. A peak DETC-NAC concentration occurred approximately 6-h after dosing (Fig. 5A). DETC-NAC was still seen in plasma 10-h after DSF dosing. In both experiments a non-zero concentration of both CARB and DETC-NAC was observed at t_0 (Fig. 5A and B). After a 62.5 mg dose of DSF (Fig. 5A), the average concentration of CARB and DETC-NAC at t_0 was 0.09 nM and 1.6 nM respectively. We believe that these concentrations of CARB and DETC-NAC are reflective of the variability typically seen in cases where the analyte concentration in a sample is close to the assay's limit of detection. After a 250 mg dose of DSF, the average t_0 concentration of CARB and DETC-NAC was even greater than that seen after the administration of a 62.5 mg of DSF (0.50 nM and 26.0 nM respectively) (Fig. 5B). This was a cross-over study and the same patients were used. Since DSF was given daily for 3 days and plasma analysis initiated on the fourth day, the DETC-NAC at t_0 appears to reflect the carry-over from the previous days dosing. This is suggested by the finding that for the 62.5 mg/day dose of DSF, the average area under the DETC-NAC curve (AUC) was 61.9 h $\mu\text{g/ml}$. For the 250 mg/day dose, the AUC was almost 8-fold higher at 483.8 h $\mu\text{g/ml}$. In both cases the average time when maximal plasma concentration achieved post administration (i.e. the T_{max}) was approximately 6-h. The ratio of the maximum DETC-NAC concentration observed (i.e. ratios of the respective C_{max}) between the two doses of

DSF was 5.6 and close to the 4-fold difference between the 62.5 and 250 mg/day dose of DSF.

3.2.6. DETC-NAC in plasma and NAC and MPFC of rats—The validated method was used to generate DETC-NAC concentration profiles as a function of time in plasma and in the NAc and mPFC of DSF-treated rats (Fig. 6). Initially, there is a lag of approximately 50 min in the plasma, NAc and mPFC before DETC-NAC increases. This delay most likely reflects both the slow absorption characteristics of DSF and the metabolism required to form DETC-NAC (Fig. 1). In both the plasma and the respective brain regions, DETC-NAC remains elevated for at least six hours. Although, there is some variability at each time point this likely reflects the variability in DSF absorption, the poor solubility of DSF in vivo, and the complexity of DSF metabolism.

3.2.7. Biological significance of the sequential appearance of CARB and DETC-NAC—This work was initiated on the suspicion that an unknown DSF metabolite had been detected in the plasma of a human volunteer [16]. In the course of developing and validating an accurate, repeatable and precise HPLC–MS/MS assay to identify and quantify this molecule, we observed pharmacokinetic phenomena consistent with the conclusion that DETC-NAC is the terminal metabolite of DSF.

Firstly, DETC-NAC consistently trails the appearance of CARB and with a longer duration in rats (Fig. 6) and humans (Fig. 5). Secondly, administration of two different doses of DSF to a patient volunteer consistently produced a peak DETC-NAC concentration 4 h after DSF dosing. Thirdly, the maximum plasma concentration of DETC-NAC after the 250 mg/day dose of DSF was approximately four times greater than that of the 62.5 mg/day dose of DSF. We conclude that DETC-NAC is a metabolite of DSF and is formed from CARB as suggested previously by Hu et al. [18].

Furthermore the juxtaposition of the appearance of CARB and DETC-NAC suggests that DETC-NAC might be responsible for neurotransmitter changes that persisted in DSF- and CARB-treated rats long after the disappearance of CARB [17]. The rat studies described above (Fig. 6) were carried out to better correlate the appearance of DETC-NAC with the timing of changes in brain neurotransmitter levels in rats treated with DSF [17]. DETC-NAC in rat plasma as well as in the NAc and mPFC rose in tandem after an initial lag period (Fig. 6) consistent with the supposition that DETC-NAC may either cause or prolong the perturbation in neurotransmitter levels seen in the previous study and attributed to the presence of CARB. The observed lag in DETC-NAC appearance relative to CARB is explained as DETC-NAC is the mercapturic acid pathway product [19] of CARB. This lag is seen in the human patient following a 62.5 mg/day dose of DSF but not after a second 250 mg/day dose. We attribute this to the fact that this was a cross-over study conducted in the same patient with an insufficient wash-out time (3-days) allotted between doses. From the present studies, we note that the lag time in the appearance of DETC-NAC is similar to the delay in changes observed in dopamine, gamma-aminobutyric acid, and glutamate levels during the microdialysis studies carried out on DSF-treated rats [17]. The correlation between CARB and DETC-NAC detected in brain regions and perturbations in neurotransmitter levels plus clinical studies suggesting DSF's efficacy in addiction therapy

requires further study. Such studies would be meritorious given the fact that various neurotransmitters including dopamine, gamma-aminobutyric acid, and glutamate have been implicated in alcohol [25], cocaine [26], and in nicotine use disorders [27] in an attempt to understand the biological basis of these addictions.

Studies over the last several decades have now shown that DSF is not a simple drug molecule but rather a pro-drug that forms a number of metabolites during its bioactivation [11,28,29] (Fig. 1). Other than the DSF metabolite DETC-MeSO, which is responsible for the inhibition of ALDH₂ [12], the pharmacological actions of the various DSF metabolites are not understood. It is only recently that the DSF metabolite CARB has been found to produce changes in dopamine, gamma-aminobutyric acid, and glutamate in the NAc and mPFC [17], two brain regions of the reward pathway. The finding of DETC-NAC in the NAc and mPFC, and in plasma of rats after DSF administration (Fig. 6) also indicates that even though mercapturic acid formation and elimination by the kidney as a detoxification process is expected [19], the observation that DETC-NAC is found in the brain of rats treated with DSF is a novel finding. DETC-NAC also is found in urine of rats after DETC-MeSO (Nagendra and Faiman unpublished results) or after DSF administration [18]. These observations coupled with our discovery of CARB [17] and DETC-NAC in the plasma of DSF-treated patients (Fig. 2A and B) suggest that CARB and DETC-NAC formation respectively may reflect a final pathway in DSF metabolism via the mercapturate pathway [19]. The enzymatic suite powering the mercapturate pathway is concentrated in the liver and kidneys with instances where mercapturate intermediates are shuttled between them via the vascular system. This could represent one explanation for the presence of both CARB and DETC-NAC in the plasma of DSF-treated mammals. The presence of CARB [17] and DETC-NAC (Fig. 5) in the NAc and mPFC of DSF-treated rats indicates that both can cross the blood–brain barrier.

4. Conclusion

In conclusion, we have developed a sensitive, selective, and robust HPLC–MS/MS method for quantitative analysis of DETC-NAC utilizing, as an internal standard, the DETC-NAC structural homolog *N*-acetyl-*S*-(*N,N*-di-isopropylcarbamoyl) cysteine. We demonstrated the effectiveness of the assay during studies of DSF-treated rats and human patients wherein DETC-NAC levels were monitored in a variety of biological matrices thereby demonstrating the flexibility of the method.

The results from the current studies are the first report identifying DETC-NAC in the plasma of human volunteers, and in the NAc, mPFC and in plasma of rats after DSF administration. Based upon these observations, it is not unreasonable to suggest that DETC-NAC also would be found in the brain of human subjects receiving DSF. These observations invite speculation about how DETC-NAC might influence neurotransmitters levels. Microdialysis studies carried out by Faiman et al. [17] demonstrated that rats dosed with DSF experience perturbations in their dopamine, gamma-aminobutyric acid and glutamate levels in the NAc and mPFC that persisted as CARB levels declined. In human studies (Fig. 5) after DSF administration, the peak appearance of CARB in plasma (Fig. 5) precedes that of DETC-NAC, and that the concentration of DETC-NAC is always greater than CARB. Furthermore

DETC-NAC in plasma is maintained while the concentration of CARB begins to return to baseline. Perturbations in the neurotransmitter levels in the brains of DSF- and CARB-treated rats persist beyond the clearance of CARB [17]. The significance of these observations in the treatment of various addictions is intriguing and remains to be established in future studies employing an animal model to establish proof of concept.

Supplementary Material

Refer to Web version on PubMed Central for supplementary material.

Acknowledgments

The Micromass Ultima was purchased with support from the KU Research Development Fund and the Acquity chromatograph with partial support from K-INBRE (www.kumc.edu/kinbre/) (TDW). This work was supported in part by grants from the National Institute on Drug Abuse of the National Institute of Health to EFM grant numbers DA 023359 and DA 024982 and to MDF grant number DA 021727.

References

1. Carroll KM, Fenton LR, Ball SA, Nich C, Frankforter TL, Shi J, Rounsaville BJ. Efficacy of disulfiram and cognitive behavior therapy in cocaine-dependent outpatients: a randomized placebo-controlled trial. *Arch Gen Psychiatry*. 2004; 61:264–272. [PubMed: 14993114]
2. Faiman MD, Kaul S, Latif SA, Williams TD, Lunte CE. *S*-(*N,N*-diethylcarbamoyl)glutathione (carbamathione), a disulfiram metabolite and its effect on nucleus accumbens and prefrontal cortex dopamine, GABA, and glutamate: a microdialysis study. *Neuropharmacology*. 2013; 75C:95–105. [PubMed: 23891816]
3. Gessner T, Jakubows M. Diethyldithiocarbamic acid methyl ester. A metabolite of disulfiram. *Biochem Pharmacol*. 1972; 21:219–230. [PubMed: 4645555]
4. Grant JE, Kim SW, Odlaug BL. *N*-acetyl cysteine, a glutamate-modulating agent, in the treatment of pathological gambling: a pilot study. *Biol Psychiatry*. 2007; 62:652–657. [PubMed: 17445781]
5. Hald J, Jacobsen E, Larsen V. The sensitizing effect of tetraethylthiuramdisulphide (antabuse) to ethylalcohol. *Acta Pharmacol Toxicol (Copenh)*. 1948; 4:285–296.
6. Hart BW, Faiman MD. In vitro and in vivo inhibition of rat liver aldehyde dehydrogenase by *S*-methyl *N,N*-diethylthiolcarbamate sulfoxide, a new metabolite of disulfiram. *Biochem Pharmacol*. 1992; 43:403–406. [PubMed: 1311578]
7. Heemskerk AA, van Haandel L, Woods JM, McCance-Katz EF, Williams TD, Stobaugh JF, Faiman MD. LC–MS/MS method for the determination of carbamathione in human plasma. *J Pharm Biomed Anal*. 2011; 54:799–806. [PubMed: 21145687]
8. Hinchman CA, Ballatori N. Glutathione conjugation and conversion to mercapturic acids can occur as an intrahepatic process. *J Toxicol Environ Health*. 1994; 41:387–409. [PubMed: 8145281]
9. Hu P, Jin L, Baillie TA. Studies on the metabolic activation of disulfiram in rat. Evidence for electrophilic *S*-oxygenated metabolites as inhibitors of aldehyde dehydrogenase and precursors of urinary *N*-acetylcysteine conjugates. *J Pharmacol Exp Ther*. 1997; 281:611–617. [PubMed: 9152363]
10. Jin L, Davis MR, Hu P, Baillie TA. Identification of novel glutathione conjugates of disulfiram and diethyldithiocarbamate in rat bile by liquid chromatography–tandem mass spectrometry. Evidence for metabolic activation of disulfiram in vivo. *Chem Res Toxicol*. 1994; 7:526–533. [PubMed: 7981417]
11. Johansson B, Angelo HR, Christensen JK, Moller IW, Ronsted P. Dose–effect relationship of disulfiram in human volunteers. 2. A study of the relation between the disulfiram–alcohol reaction and plasma-concentrations of acetaldehyde, diethyldithiocarbamic acid methyl-ester, and erythrocyte aldehyde dehydrogenase-activity. *Pharmacol Toxicol*. 1991; 68:166–170. [PubMed: 1647526]

12. Kaul S, Faiman MD, Lunte CE. Determination of GABA, glutamate and carbamathione in brain microdialysis samples by capillary electrophoresis with fluorescence detection. *Electrophoresis*. 2011; 32:284–291. [PubMed: 21254127]
13. Kaul S, Williams TD, Lunte CE, Faiman MD. LC–MS/MS determination of carbamathione in microdialysis samples from rat brain and plasma. *J Pharm Biomed Anal*. 2010; 51:186–191. [PubMed: 19709836]
14. Madan A, Parkinson A, Faiman MD. Identification of the human and rat P450 enzymes responsible for the sulfoxidation of *S*-methyl *N,N*-diethylthiocarbamate (DETC-ME). The terminal step in the bioactivation of disulfiram. *Drug Metab Dispos*. 1995; 23:1153–1162. [PubMed: 8654205]
15. Mutschler J, Buhler M, Grosshans M, Diehl A, Mann K, Kiefer F. Disulfiram, an option for the treatment of pathological gambling? *Alcohol Alcohol*. 2010; 45:214–216. [PubMed: 20083479]
16. Nagendra SN, Faiman MD, Davis K, Wu JY, Newby X, Schloss JV. Carbamoylation of brain glutamate receptors by a disulfiram metabolite. *J Biol Chem*. 1997; 272:24247–24251. [PubMed: 9305877]
17. Paxinos, G.; Watson, C. *The Rat Brain in Stereotaxic Coordinates*. 2nd. Academic Press; Sydney/Orlando: 1986.
18. Yourick JJ, Faiman MD. Comparative aspects of disulfiram and its metabolites in the disulfiram–ethanol reaction in the rat. *Biochem Pharmacol*. 1989; 38:413–421. [PubMed: 2537080]
19. Yourick JJ, Faiman MD. Disulfiram metabolism as a requirement for the inhibition of rat-liver mitochondrial low *K_m* aldehyde dehydrogenase. *Biochem Pharmacol*. 1991; 42:1361–1366. [PubMed: 1656985]

Abbreviations

ALDH₂	aldehyde dehydrogenase
AUC	area under the curve
CARB	carbamathione/ <i>S</i> -(<i>N,N</i> -diethylcarbamoyl) glutathione
DSF	disulfiram
DDTC	diethyldithiocarbamate
DDTC-Me	<i>S</i> -methyl- <i>N,N</i> -diethyldithiocarbamate
DDTC-MeSO	<i>S</i> -methyl- <i>N,N</i> -diethyldithiocarbamate sulfoxide
DDTC-MeSO₂	<i>S</i> -methyl- <i>N,N</i> -diethyldithiocarbamate sulfone
DETC-Me	<i>S</i> -methyl- <i>N,N</i> -diethylthiocarbamate
DETC-MeSO	<i>S</i> -methyl- <i>N,N</i> -diethylthiocarbamate sulfoxide
DETC-MeSO₂	<i>S</i> -methyl- <i>N,N</i> -diethylthiocarbamate sulfone
DETC-NAC	<i>N</i> -acetyl- <i>S</i> -(<i>N,N</i> -diethylcarbamoyl) cysteine
DIPC-NAC	<i>N</i> -acetyl- <i>S</i> -(<i>N,N</i> -di-isopropylcarbamoyl) cysteine
HPLC–UV	HPLC with UV detection
mPFC	medial prefrontal cortex
NAc	nucleus accumbens
<i>t</i>₀	zero time

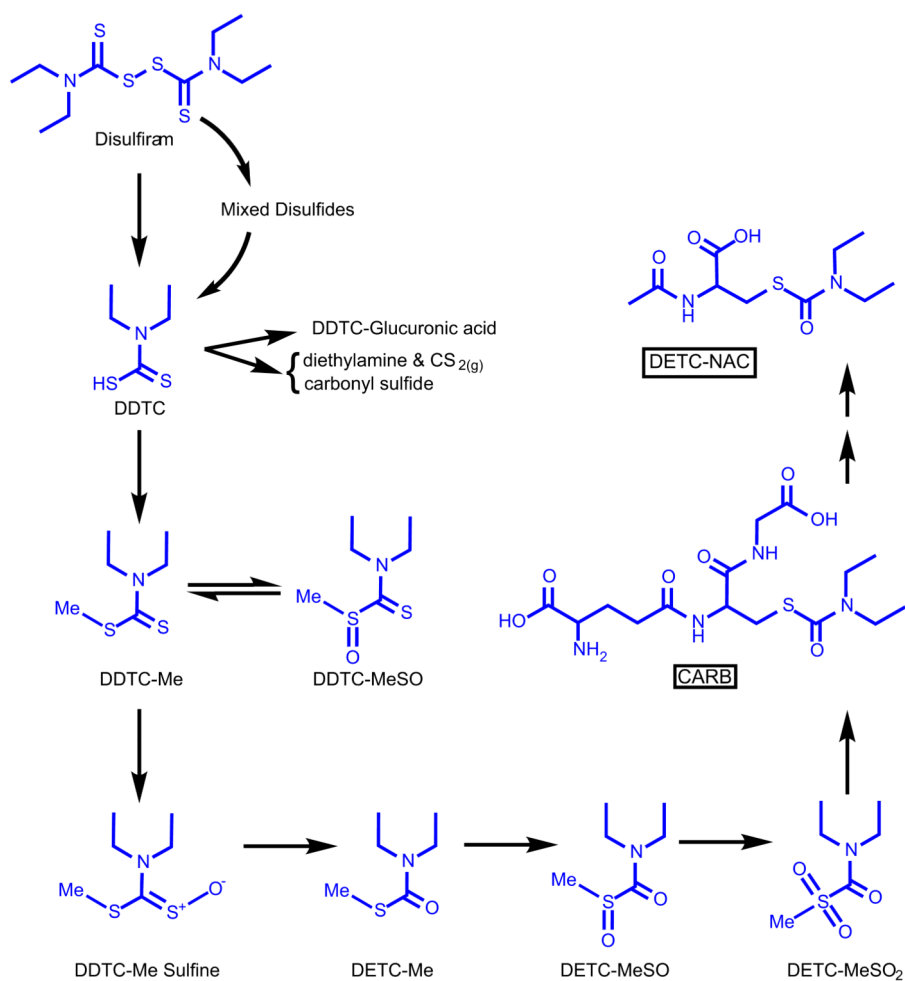


Fig. 1.
The bioactivation of DSF.

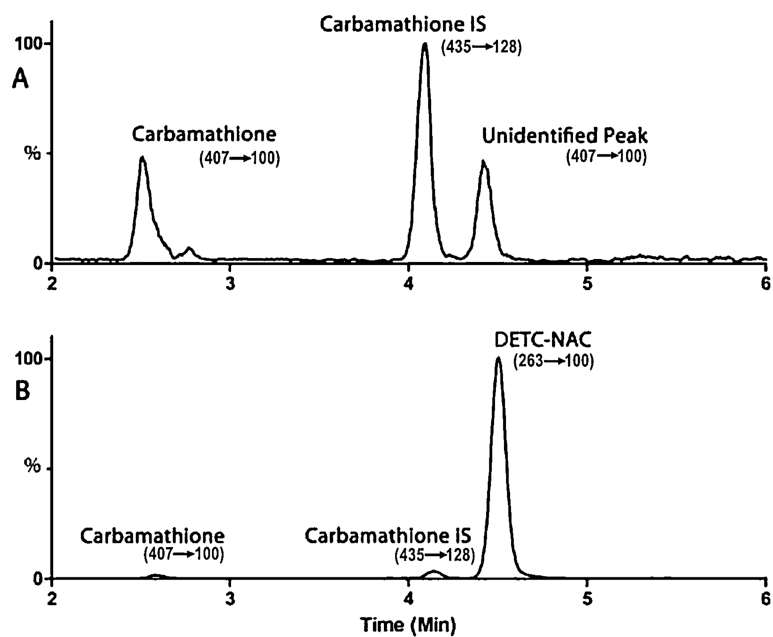


Fig. 2. Identification of DETC-NAC in human plasma. The unknown peak previously found at a transition of 407 → 100 u upon analysis of human plasma [16] (Fig. 2A), is identified as DETC-NAC (Fig. 2B) the transition is MH^+ to carbamoyl fragment observed in Fig. 3.

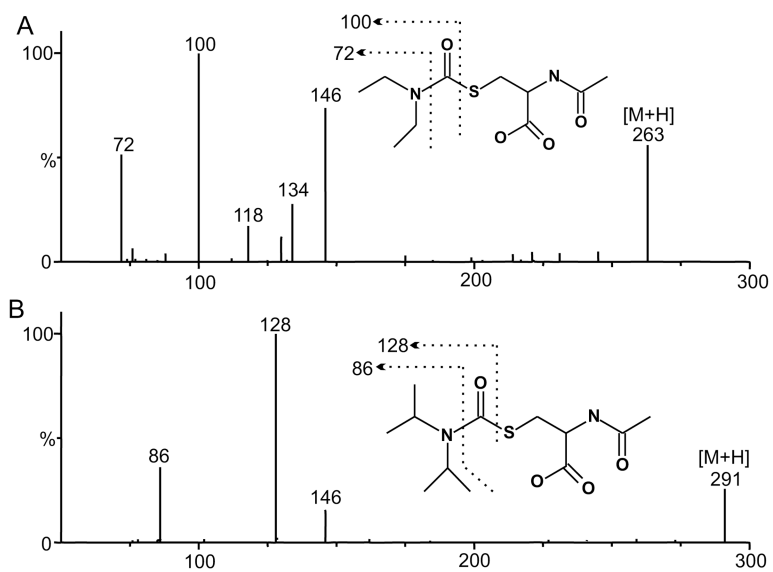


Fig. 3. Fragmentation of DETC-NAC (A) and the internal standard DIPC-NAC (B) with the 100 m/z and 128 m/z fragments used in MIM indicated.

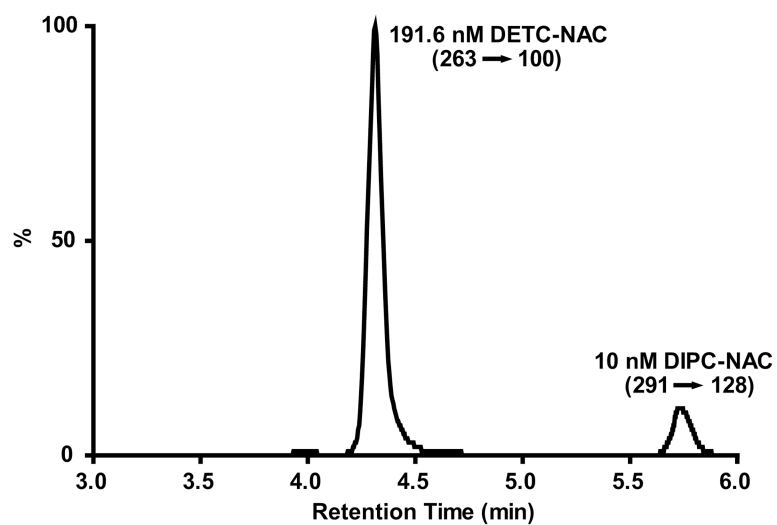


Fig. 4. HPLC–MS/MS (selected reaction monitoring) elution profile of typical chromatographic resolution and detection of DETC-NAC and DIPC-NAC in the plasma samples from a 53 year old female volunteer dosed with 250 mg DSF (see human studies).

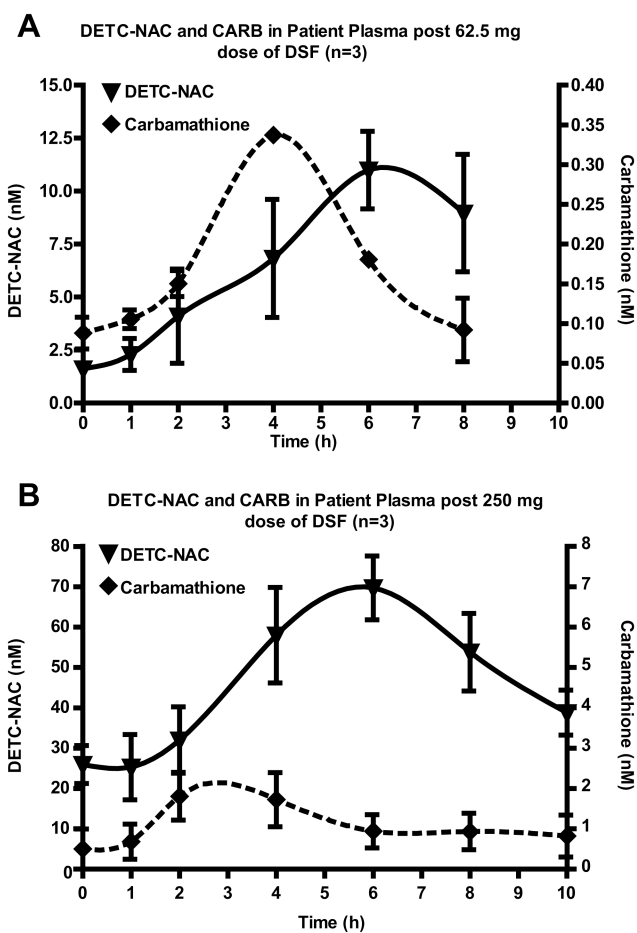


Fig. 5. The concentration profiles of DETC-NAC and CARB in the plasma of a human volunteer following an oral dose of (A) 62.5 mg DSF followed by a 3 day delay then (B) a 250 mg DSF dose. Error bars show the standard error of the mean.

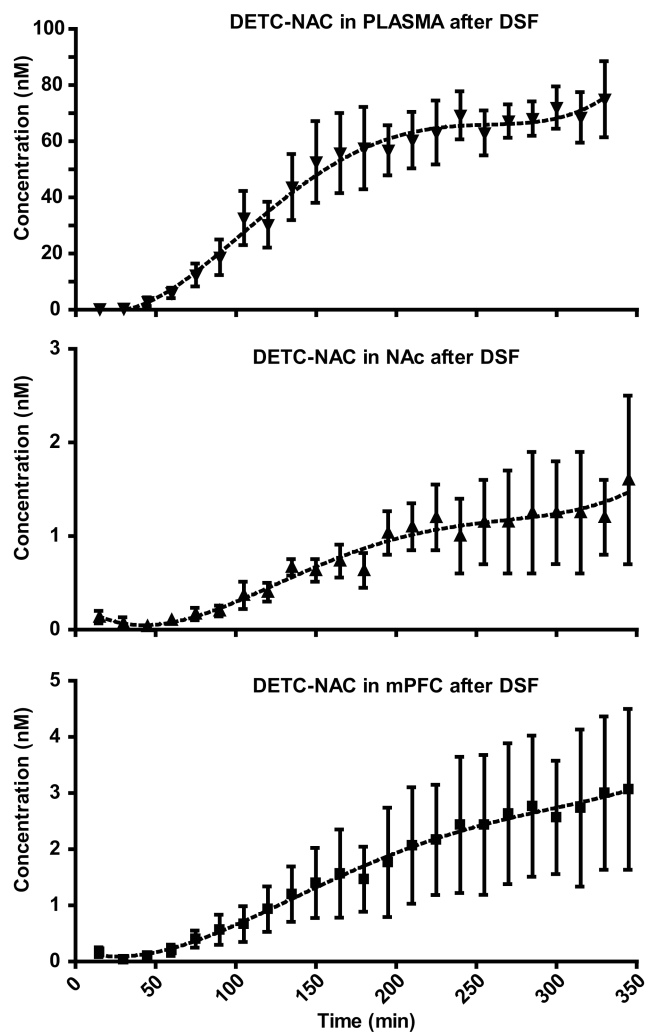


Fig. 6. Concentrations of DETC-NAC in the plasma, NAc and mPFC of rats ($n = 3$) after dosing with DSF (200 mg/kg, intraperitoneal). Error bars show the standard error of the mean.